Faraday Discuss., 1997, **106**, 377–387

Free energy of formation of defects in polar solids

M. B. Taylor,[a] G. D. Barrera,[a] N. L. Allan,[a]*,† T. H. K. Barron[a] and W. C. Mackrodt[b]

[a] *School of Chemistry, University of Bristol, Cantock's Close, Bristol, UK BS8 1TS*
[b] *School of Chemistry, University of St. Andrews, St. Andrews, Fife, UK KY16 9ST*

A more exact method than hitherto available, based on lattice statics and quasi-harmonic lattice dynamics, is presented for the direct minimisation of the free energies of periodic solids with very large unit cells. This is achieved *via* the calculation of analytic derivatives of the vibrational frequencies with respect to all external and internal variables. The method, together with large defective supercells, is used to calculate the free energies of defects in MgO as a function of temperature. A major advantage of the supercell approach is that constant-volume and constant-pressure quantities are calculated independently. This allows a critical appraisal of the common approximations used for many years: (i) to convert constant-volume defect parameters to constant-pressure and (ii) to justify the use of static calculations at constant volume in the interpretation of experimental data obtained at constant pressure and at high temperatures. Defect enthalpies show only a small variation with temperature and differ by *ca.* 2% from the internal energy change in the static limit. An assessment is also made of the commonly used ZSISA approximation, in which the free energy at each temperature is minimised with respect to external strains only, simultaneously determining the internal strains by minimising the static lattice energy.

The modelling of complex solids, such as crystals with large unit cells, crystals with defects, and surfaces, presents severe computational demands if reasonably high precision is required. Quasi-harmonic lattice dynamics, in principle, give high precision, and in many applications have been shown to be a valid approximation up to two-thirds of the melting temperature.[1] In Bristol, we are developing a code designed for the efficient study of periodic structures with internal strains. Following successful applications to relatively simple systems,[2] we are now ready for applications to structures with many independent internal strains and, to illustrate the method, in this paper we present results for defect free energies in MgO.

Point-defect energies in polar solids have been extensively studied for many years, leading to considerable insight into complex defect phenomena in a wide range of systems.[3–5] As elsewhere in computational solid-state physics and chemistry, the majority of point-defect calculations have assumed zero temperature and, for the most part, have involved the evaluation of the static part of the internal energy change accompanying defect formation only at constant volume.[6] Furthermore, even though the vast majority of experimental data has been obtained at elevated temperatures and constant pressure, almost invariably these have been compared with static internal energies calculated at constant volume. Clearly, this procedure is questionable, other than for specific data such as the migration energy of point defects, which are most appropriately compared with values calculated at 0 K. Accordingly, we employ our new computational

† E-mail: n.l.allan@bris.ac.uk

methods to calculate free energies of defect formation, so that we can make a critical appraisal of the approximations commonly used to justify comparisons of calculated and experimental defect quantities.

It has been known for some time that the use of 'supercells' to describe a defective lattice, together with the quasi-harmonic approximation, provides a convenient approach to the calculation of defect free energies.[7] In this method, a superlattice of defects is introduced, extending throughout the macroscopic crystal. The periodicity is then of the superlattice and the supercell contains many atoms whose equilibrium positions are not wholly determined by symmetry, but are described by a set of dimensionless internal strain coordinates ε_k. Defect properties, such as energies and entropies,‡ can then be computed both at constant pressure and at constant volume, *e.g.*

$$g_p = g_p(P, T) = \{G_{\mathrm{dc}}(P, T) - G_{\mathrm{pc}}(P, T)\}/N_{\mathrm{d}} \quad (1)$$

$$f_v = f_v(V, T) = \{F_{\mathrm{dc}}(V, T) - G_{\mathrm{pc}}(V, T)\}/N_{\mathrm{d}} \quad (2)$$

where G_{dc} and G_{pc}, F_{dc} and F_{pc} are free energies of the macroscopic defect crystal and perfect crystal, respectively, and N_{d} is the total number of defects introduced into the macroscopic crystal.§ Convergence towards properties of an isolated defect occurs as the superlattice spacing is increased.

In the quasi-harmonic approximation, the vibrational frequencies are explicit functions of the crystallographic parameters but not of the temperature. Within this scheme the free energy is obtained by simultaneous direct minimisation with respect to both external (η_λ) and internal (ε_k) strains. For the most part, however, previous calculations[8,9] have been based on a widely used approximation, ZSISA (zero static internal stress approximation), which is computationally more tractable than the full minimisation. In this approximation the free energy is minimised with respect to η_λ only, subject to the condition that the (static) internal energy is minimised with respect to the internal strains ε_k for each state of external strain. In this paper we present defect free energies which have been obtained without resorting to the ZSISA approximation. To our knowledge this is the first report based on the full minimisation.

Other approaches to the calculation of defect free energies have included the use of the perfect-lattice Green's function, in conjunction with changes in the lattice force constant resulting from the presence of the defect.[10] The difficulties associated with the computational implementation of this approach appear to more than outweigh its formal elegance. A 'large-crystallite' method has also been developed by Harding,[11,12] which is an 'embedding' approach and the analogue of the widely used two-region approach to static defect energies:[13] in the inner region, which contains the defect, the ions are allowed to vibrate, while in the outer region they are held fixed. However, in neither of these two approaches are defect free energies calculated at constant pressure. The principal advantage of the supercell method implemented in the present work, therefore, is that enthalpies and entropies at elevated temperatures and constant pressure can be evaluated directly.

In this paper we concentrate on point-defects in MgO and, in particular, the substitution of Mg^{2+} by Ba^{2+}, which involves a large structural distortion of the lattice since the Ba^{2+} ion is so much larger than Mg^{2+}. Our primary aim is to demonstrate the methodology and to give a critical appraisal of various approximations and assumptions that have been employed in earlier work. Applications to further defects and more complex systems will be reported separately.

‡ We denote defect quantities by lower case letters, *e.g.* g_p denotes the change in Gibbs energy at constant pressure.

§ This does not, of course, include the configurational entropy of a dilute solution of randomly positioned defects.

Theoretical methods

In the quasi-harmonic approximation it is assumed that the Helmholtz energy of a crystal, F, at a temperature T can be written as the sum of static and vibrational contributions,

$$F(\mathscr{E}, T) = \Phi_{\text{stat}}(\mathscr{E}) + F_{\text{vib}}(\mathscr{E}, T) \tag{3}$$

Φ_{stat} is the potential energy of the static lattice in a given state of strain $\mathscr{E}$, and F_{vib} is the sum of harmonic vibrational contributions from all the normal modes. For a periodic structure, the frequencies $\nu_j(\boldsymbol{q})$ of modes with wavevector $\boldsymbol{q}$ are obtained by diagonalisation of the dynamical $D(\boldsymbol{q})$ in the usual way,[14] so that F_{vib} is given by

$$F_{\text{vib}} = \sum_{q,\,j} (\tfrac{1}{2}h\nu_j(\boldsymbol{q}) + k_{\text{B}}\,T\,\ln\{1 - \exp[-h\nu_j(\boldsymbol{q})/k_{\text{B}}\,T]\}) \tag{4}$$

where the first term is the zero-point energy at $T = 0$. For a macroscopic crystal the sum over $\boldsymbol{q}$ becomes an integral over a cell in reciprocal space, which can be evaluated by taking successively finer uniform grids[15] until convergence is achieved.[16] The Helmholtz energy thus obtained is a function of both macroscopic (η_λ) and internal strains (ε_k), and it is simplest to treat the ε_k as thermodynamic variables on the same footing as the η_λ, comprising a total set of strain variables[17,18] denoted by $\mathscr{E}_{\text{A}}$. The equilibrium structure at an applied pressure P is then that which minimises the availability[19] $F + PV$ with respect to all strains. As in the static simulation of point defects the number of independent degrees of freedom can often be reduced substantially by symmetry considerations.

There are now two ways of proceeding. The minimisation of $F + PV$ and subsequent thermodynamic manipulation can of course be carried out by brute force, from numerical values of F obtained using eqn. (4). However, for large unit cells with many internal strains, it can be much more efficient to use analytic expressions for the derivatives of F with respect to temperature and strain. Not only does this give explicit expressions for thermodynamic properties, such as

$$S = \sum_{q,\,j} \frac{[h\nu(\boldsymbol{q})/T]}{\exp[h\nu_j(\boldsymbol{q})/k_{\text{B}}\,T] - 1} - k\,\ln\{1 - \exp[-h\nu_j(\boldsymbol{q})/k_{\text{B}}\,T]\} \tag{5}$$

which can readily be evaluated to a high precision; also, the strain derivatives permit a more rapid minimisation of $F + PV$. The strain derivatives (which give the stresses $\mathscr{T}_{\text{A}}$ conjugate to the $\mathscr{E}_{\text{A}}$) are given by

$$\left(\frac{\partial F_{\text{vib}}}{\partial \mathscr{E}_{\text{A}}}\right)_{\mathscr{E}',\,T} = V\mathscr{T}_{\text{A}} = \sum_{q,\,j} \left\{\frac{h}{2\nu_j(\boldsymbol{q})}\left(\frac{1}{2} + \frac{1}{\exp[h\nu_j(\boldsymbol{q})/k_{\text{B}}\,T] - 1}\right)\left(\frac{\partial \nu_j^2(\boldsymbol{q})}{\partial \mathscr{E}_{\text{A}}}\right)_{\mathscr{E}'}\right\} \tag{6}$$

where the subscripts $\mathscr{E}'$ denote that all the $\mathscr{E}$ are kept constant except for the differentiation variable. We thus require derivatives of the frequencies. In our new code the derivatives $[\partial\nu_j^2(\boldsymbol{q})/\partial\mathscr{E}_{\text{A}}]_{\mathscr{E}'}$ are obtained from the analytic expressions for the derivatives $(\partial D/\partial\mathscr{E}_{\text{A}})_{\mathscr{E}'}$ by first-order perturbation theory.[14,20–22] A crucial point here is that, for obtaining derivatives, the perturbation is infinitesimal and so the procedure is exact. Furthermore, for thermodynamic properties no special consideration need be given to degeneracies in first-order perturbation theory, since the trace of $(\partial D/\partial\mathscr{E}_{\text{A}})_{\mathscr{E}'}$ is invariant for any complete normal set of eigenvectors of D. Results obtained in this way are in excellent agreement with those derived from numerical derivatives of $F + PV$ using finite increments of 10^{-5} in $\mathscr{E}_{\text{A}}$.

To obtain the equilibrium structure and Gibbs energy our new code uses a variable metric method[23] for minimising $F + PV$ with respect to $\mathscr{E}_{\text{A}}$. In the initial configuration the static energy Hessian, $(\partial^2\Phi_{\text{stat}}/\partial\mathscr{E}_{\text{A}}\,\partial\mathscr{E}_{\text{B}})$, which is a good approximation to $(\partial^2 F/\partial\mathscr{E}_{\text{A}}\partial\mathscr{E}_{\text{B}})$,

is calculated from its analytic expression, and its inverse, together with $(\partial F/\partial \mathscr{E}_A)$, is used to obtain an improved configuration. In subsequent iterations $(\partial F/\partial \mathscr{E}_A)$ are calculated in the new configurations and the inverse Hessian updated by the BFGS formula.[24]

There remains the question of the validity of the quasi-harmonic approximation, which breaks down with increasing internuclear separations and, hence, at high temperatures. This can be investigated either by computing terms in the lattice dynamics of higher order in the anharmonicity, or more commonly by classical Monte Carlo or molecular dynamics simulations. Previous work[25] on the bulk properties of MgO has shown that, using the same potential as here, the quasi-harmonic approximation is valid up to temperatures of approximately two-thirds of the melting point (3100 K). Accordingly, here we consider a range of temperatures 0–1500 K.

Defect thermodynamics

The chief quantities of interest are the free energy changes accompanying defect formation at constant volume (f_v) and at constant pressure (g_p), defined in eqn. (1) and (2). To calculate f_v, the external strain is kept constant while the internal degrees of freedom are varied to give the equilibrium configuration. Similarly, for g_p, both external and internal strains are varied, to be consistent with the specified pressure. It is also straightforward to determine the defect enthalpy, h_p and the entropy change at constant pressure, s_p, from the various terms that contribute to the free energy of these cells. The volume of formation of the defect, v_p, follows immediately from the minimisation of $F + PV$.

Several relations between defect properties evaluated at constant pressure and at constant volume have been given by Catlow *et al.*[26] These are strictly valid only in the limit when $(v_p/V) \to 0$, *i.e.* when a single defect is added to a macroscopic crystal. In this limit, constant pressure quantities can be derived from those obtained at constant volume:

$$g_p = f_v \tag{7}$$

$$h_p = u_v + (\beta T/\kappa_T)v_p \tag{8}$$

$$s_p = s_v + (\beta/\kappa_T)v_p \tag{9}$$

where β is the volumetric thermal expansion coefficient, κ_T the isothermal compressibility and v_p is itself given by

$$v_p = \kappa_T V p_v = -\kappa_T V\left(\frac{\partial f_v}{\partial V}\right)_T \tag{10}$$

In some studies[27,28] $(\partial u_v/\partial V)_T$ has been used as an approximation to $(\partial f_v/\partial V)_T$.

A major advantage of our supercell approach is that we are able to calculate all these quantities independently, notably those at constant pressure. This is important because, in supercell computations, the relative change of volume is $(v_p/v_{\text{supercell}})$, which is finite for the superlattices used. Our results can, therefore, be used to investigate not only the validity of approximations such as $h_p(T) \approx u_v(0)$, but also departures from relationships such as $g_p = f_v$. The first-order correction to eqn. (7) is given by

$$f_v - g_p = \frac{1}{2}\left(\frac{v_p}{\kappa_T}\right)\left(\frac{v_p}{v_{\text{supercell}}}\right) \tag{11}$$

The physical reason for this correction is that, whereas an isolated defect introduced at constant volume into a macroscopic crystal is embedded in surroundings effectively at zero pressure, the defect in the supercell is embedded in surroundings at pressure $p_v = (v_p/\kappa_T)v_{\text{supercell}}$. We may, therefore, expect $f_v - \frac{1}{2}(v_p/\kappa_T)(v_p/v_{\text{supercell}})$ to be a better estimate of the value of f_v for an isolated defect.

The traditional identification of the measured defect enthalpy at temperature T, $h_p(T)$, with the internal energy change at $T = 0$, $u_v(0)$, has been justified[12] by expanding $h_p(T)$ as a power series in T about $T = 0$, with a vanishing term in T and non-vanishing term in T^2. Since, for a real non-metallic quantum crystal, h_p varies as T^4 at low temperatures, this is clearly a classical argument, and so valid only for $T > \Theta_D$ and then only when higher anharmonic terms are small; moreover, classically the defect internal energy at $T = 0$ is u_v(static). Thus while $u_v(0)$ is a better approximation for $h_p(T)$ at sufficiently low temperatures, u_v(static) may be better for $T > \Theta_D$.

Results and Discussion

In this section we report results for the barium substitutional defect in MgO, Ba^x_{Mg}. This gives rise to a greater elastic relaxation than does any other simple point defect, thus posing an extremely stringent test of the supercell approach and the methodology we have developed. All the calculations are based on the consistent set of interatomic Buckingham potentials reported by Sangster and Stoneham.[29] In the present application, cubic symmetry is preserved if the Ba^{2+} superlattice is itself cubic: face-centred cubic (fcc), body-centred cubic (bcc) or simple cubic (sc). The possibilities for Ba mole fractions down to *ca.* 0.3% are listed in Table 1. Of these, we might expect results obtained from fcc supercells to converge most rapidly, both because for a given mole fraction the defects are further away from each other and because the nearest neighbour shell of 12 defects gives an environment more like the isotropic environment of an isolated defect.

Table 2 lists the results in the static limit for the defect volumes, v_p, internal energies, u_v, and enthalpies, h_p, as a function of unit cell size, from which it appears that the convergence with unit cell size is somewhat irregular. For example, the 54-ion supercells (fcc) give a value closer to that in the dilute limit than 64-ion supercells (cub). However, the convergence is consistent for the same type of supercell, and as expected the fastest convergence is obtained for the fcc supercells. This is true also of the temperature-dependent properties calculated (Table 3 and Fig. 1).

For a correct calculation at $T = 0$ we must include the zero-point energy, which expands the lattice and changes the defect parameters. For this reason, Table 2 also contains 0 K values of v_p, u_v, and h_p. For supercells of the same size, the values of h_p and u_v are lower than the static value by *ca.* 0.2 eV from the static value, while v_p is higher by *ca.* 1%.

We have carried out full minimisations of F and $F + PV$ for each of the supercells at three temperatures in the range 500–1500 K. The resulting defect constant-pressure and constant-volume parameters are listed in Table 3. Over the temperature range 500–1500 K, v_p, h_p and s_p increase by *ca.* 20%, *ca.* 2% and 30%, respectively; g_p, f_v and u_v all decrease by *ca.* 6% and s_v by *ca.* 30%.

As might have been expected, the defect entropies, s_v and s_p, particularly s_p, show a slower convergence with supercell size than defect energies, since the rate of convergence

Table 1 Shape of the supercells used in this paper

number of ions	mole fraction Ba	supercell shape	number of ions	mole fraction Ba	supercell shape
8	0.25	cub	216	0.0093	cub
16	0.125	fcc	250	0.0080	fcc
32	0.0625	bcc	256	0.0078	bcc
54	0.0370	fcc	432	0.0046	fcc
64	0.0313	cub	512	0.0039	cub
128	0.0156	fcc	686	0.0029	fcc

Table 2 Defect parameters for a barium substitutional defect in MgO: (i) in the static limit (ii) at 0 K including the effect of zero-point energy

	static limit			0 K		
x^a	v_p/Å^3	$g_p(=h_p)$/eV	$f_v(=u_v)$/eV	v_p/Å^3	$g_p(=h_p)$/eV	$f_v(=u_v)$/eV
32	20.9	15.559	16.520	21.1	15.354	16.304
54	20.3	16.002	16.545	20.5	15.798	16.335
64	21.4	15.819	16.326	21.6	15.609	16.113
128	20.1	15.980	16.193	20.4	15.787	15.997
216	20.3	15.898	16.030	20.6	15.733	15.839
250	20.1	15.957	16.069	20.4	15.807	15.874
256	20.0	15.920	16.028	20.3	15.772	15.835
432	20.0	15.956	16.020			
512	20.1	15.939	15.994			
686	20.0	15.960	15.999			

[a] x denotes the total number of ions in the unit cell $BaMg_{x/2-1}O_{x/2}$.

is determined by changes in the second derivative of the interatomic potential, which are more sensitive to small structural changes, such as the lattice relaxation around a defect, than the potential energy itself. s_v is small, because the entropy depends solely on the vibrational frequencies [eqn. (5)] and there are two opposite effects competing. Inserting the larger Ba^{2+} ions into the Mg^{2+} cavity at constant volume causes a small increase in pressure p_v over the whole crystal, so that the force constants become stronger and the vibrational frequencies are increased; however, the heavier mass of the Ba^{2+} ion tends to decrease frequencies. For s_p, however, the pressure is relaxed to zero and the mass effect is dominant. The absolute change in s_p with temperature is also larger than that of s_v and opposite in sign.

We consider next the behaviour of $h_p(T)$ and $u_v(T)$ and the validity of the approximations $h_p(T) \approx u_v(0)$ or u_v(static). Fig. 2 shows the variation of h_p and u_v with temperature. Above $T = 0$, $h_p(T)$ is always greater than $u_v(T)$; in the isolated defect limit, it

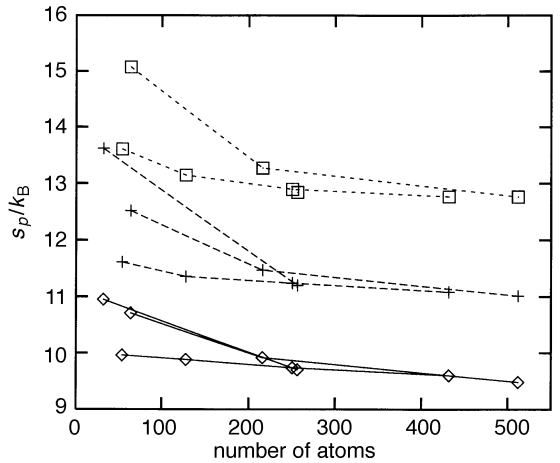

Fig. 1 Variation of s_p with unit cell size for a barium substitutional defect in MgO over a range of temperatures. At each temperature lines connect values obtained using the same shape of supercell. 500 K (◇); 1000 K (+); 1500 K (□).

Table 3 Defect volumes, energies and entropies of formation for a barium substitutional defect in MgO at 500, 1000 and 1500 K, obtained by full minimisation of the Gibbs energy

T/K	x^a	v_p/Å^3	g_p/eV	f_v/eV	h_p/eV	u_v/eV	s_p/k_B	s_v/k_B
500	32	22.4	15.034	16.026	15.506	16.080	10.95	1.27
	54	21.5	15.496	16.064	15.925	16.107	9.96	0.99
	64	22.7	15.285	15.813	15.746	15.864	10.71	1.20
	128	21.2	15.466	15.700	15.892	15.744	9.89	1.02
	216	21.5	15.391	15.523	15.819	15.569	9.92	1.08
	250	21.2	15.457	15.572	15.876	15.617	9.74	1.05
	256	21.1	15.417	15.530	15.835	15.578	9.71	1.10
	432	21.0	15.456		15.870		9.60	
	512	21.2	15.443		15.852		9.48	
1000	32	25.5	14.508	15.560	15.682	15.647	13.62	1.01
	54	23.3	15.028	15.622	16.028	15.683	11.61	0.71
	64	24.8	14.782	15.342	15.861	15.417	12.51	0.88
	128	22.9	15.009	15.265	15.987	15.329	11.36	0.74
	216	23.2	14.932	15.082	15.920	15.151	11.47	0.80
	250	22.8	15.008	15.135	15.976	15.202	11.24	0.78
	256	22.7	14.972	15.094	15.937	15.166	11.20	0.83
	432	22.6	15.017		15.972		11.08	
	512	22.8	15.010		15.959		11.01	
1500	32	—	—	15.036	—	15.155	—	0.92
	54	26.4	14.496	15.123	16.255	15.198	13.61	0.59
	64	28.7	14.195	14.811	16.143	14.907	15.07	0.74
	128	25.5	14.476	14.762	16.176	14.844	13.15	0.64
	216	26.0	14.403	14.569	16.118	14.663	13.27	0.73
	250	25.4	14.491	14.629	16.158	14.718	12.90	0.69
	256	25.3	14.457	14.591	16.117	14.690	12.84	0.76
	432	25.2	14.503		16.154		12.77	
	512	25.5	14.498		16.147		12.76	

[a] x denotes the total number of ions in the unit cell $BaMg_{x/2-1}O_{x/2}$.

follows from eqn. (7) and (9) that

$$h_p - u_v = T(s_p - s_v) = (\beta T/\kappa_T)v_p$$

and, in the present application, both v_p and β are positive. The temperature dependence of u_v is much greater than that of h_p and opposite in sign. This is a similar trend to that shown by the defect entropies, but the percentage differences are less marked because h_p and u_v are dominated by the static contributions. The results confirm that $u_v(0)$ and u_v(static) are fair approximations to $h_p(T)$, with u_v(static) a better approximation when $T > \Theta_D$. While the high-temperature values of u_v clearly extrapolate back towards u_v(static), the same is not true of h_p.

The convergence of f_v, and hence of $u_v(0)$ and u_v(static) towards their values in the dilute limit, is improved using eqn. (11). Detailed examination shows that the computed differences in $f_v - g_p$ are approximately proportional to $(v_p/v_{\text{supercell}})$ and that the expression for $f_v - g_p$ given in eqn. (11) is accurate to within *ca.* 10%. The slow convergence of f_v with increasing supercell size is thus seen to be largely due to the term $\frac{1}{2}p_v v_p$, which could be subtracted from the values for f_v obtained for each supercell size. It also calls into question the uncritical use of eqn. (7) when comparing experimental results with data calculated even with quite large supercells.

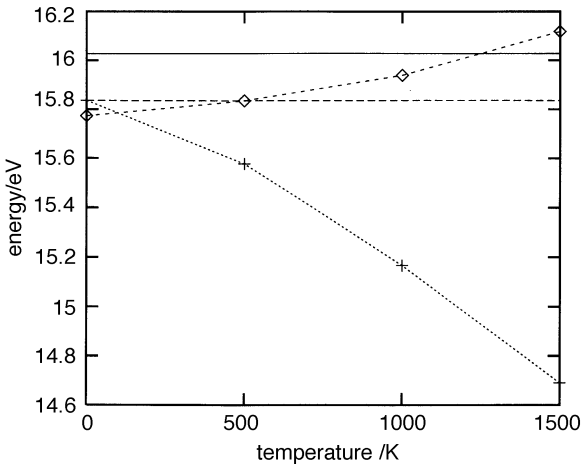

Fig. 2 Variation of h_p ($\diamond$) and u_v (+) with temperature for a supercell containing 216 ions. For comparison $u_v(0)$ (– – –) and u_v(static) (——) are also shown.

While eqn. (8) and (9) are also exact in the dilute limit, they too are often used uncritically. To investigate the potential inaccuracy that might result from such usage, we have used eqn. (9) to estimate values of s_p, at 1500 K for a range of supercells, from the corresponding values of s_v. Eqn. (9) also requires β, κ_T and v_p, and calculated values of these for MgO based on the same set of potentials are given in Table 4. Table 5 lists the resulting values of s_p, together with those determined from the direct minimisation of G. As the supercell size increases, the differences between the values in the two columns of Table 5 decrease as expected. For the 54 and 128 atom supercells (3.7% and

Table 4 Calculated bulk properties of MgO needed for eqn. (8) and (9)

	temperature/K		
property	500	1000	1500
V/Å^3	19.1593	19.4433	19.7835
$\beta/10^{-5}$ K^{-1}	2.621	3.207	3.765
$\kappa_T/10^{-3}$ GPa^{-1}	4.649	5.084	5.711

The volume given is that for a primitive unit cell.

Table 5 Comparison of methods for calculating s_p at 1500 K as a function of supercell size

	s_p/k_B	
x	eqn. (9)	full minimisation
54	11.36	13.61
128	12.81	13.15
216	13.14	13.27

Table 6 A comparison of defect volumes, and constant pressure energies and entropies of formation for a barium substitutional defect in MgO at 1500 K, obtained by full minimisation of the Gibbs energy, and the ZSISA and CISPA approximations with a supercell of 216 ions

method	v_p/Å^3	g_p/eV	h_p/eV	s_p/k_B
full minimisation	26.0	14.403	16.118	13.27
ZSISA	25.6	14.408	16.088	12.99
CISPA	24.8	14.433	16.056	12.55

1.6% Ba, respectively) there are substantial differences between the approximate value in the first column of Table 5, and that found directly by the full minimisation of the Gibbs energy.

Finally, in this section, we comment on a common approximation used in lattice dynamics at elevated temperatures, namely, the ZSISA.[30] In determinations of equilibrium structures, this approximation can reduce the computational effort considerably. The Gibbs energy at each temperature is minimised with respect to external strains only. Simultaneously the internal strains are determined by minimising the static lattice energy, and so

$$\left(\frac{\partial G}{\partial \eta_i}\right)_{\eta', \varepsilon} = \left(\frac{\partial \Phi_{\text{stat}}}{\partial \varepsilon_i}\right)_{\eta, \varepsilon'} = 0$$

Although this may give an incorrect internal strain, it gives, to first order, the correct external strain at each temperature. An even less rigorous approximation is the constant internal strain parameter approximation (CISPA), which fixes the internal strains at those calculated in the static limit; with our choice of internal strain coordinates, CISPA thus requires that the fractional coordinates of the basis atoms do not vary with temperature.

The use of ZSISA or CISPA makes no qualitative difference to any of the trends discussed in this paper. Small quantitative differences, however, are found at elevated temperatures, as shown for $T = 1500$ K in Table 6. As expected, the ZSISA results are closer to those from the full minimisation than CISPA. However, even the CISPA values for g_p and h_p differ by less than *ca.* 0.5% from the full minimisation results. In contrast, the differences between CISPA and the full minimisation results for v_p and s_p are somewhat greater at *ca.* 4 and *ca.* 5%, respectively. This calls for some caution in the use of the ZSISA and CISPA results for these quantities.

Final remarks

We have presented a more exact method than hitherto available for the direct minimisation of the free energies of periodic solids with very large unit cells, with respect to both external and internal strains. In common with previous methods,[7] it is based on lattice statics and quasi-harmonic lattice dynamics, but derives its extra rigour and flexibility from its use of analytic derivatives of the vibrational frequencies with respect to all external and internal variables. We have used it to calculate constant-pressure free energies and entropies of the barium substitutional defect in MgO, Ba^{x}_{Mg}, from 500–1500 K at defect concentrations an order of magnitude less than any previous calculations. It has also allowed us to assess the validity of two widely-used approximations in computational defect thermodynamics, ZSISA and CISPA. The proven flexibility of

this new approach will enable us to examine more complicated defects such as the 4 : 1 complex in $Fe_{1-x}O$ and to calculate important ceramic data such as phase diagrams.

We conclude with a few remarks concerning the use of lattice dynamics, which has been somewhat neglected in recent years. It has been shown previously[1,2,31] that there is good agreement up to about two-thirds of the melting point between lattice dynamics and molecular dynamics calculations based on identical potentials for properties such as the thermal expansion. It is clear from these studies and the present paper that quasi-harmonic lattice dynamics can be a useful technique for studying systems, even at quite elevated temperatures, particularly bearing in mind that to obtain comparable precision from molecular dynamics and Monte Carlo simulations can be orders of magnitude more expensive. Reasons for the utility of lattice dynamics for problems such as that considered here are that the results are often simpler to interpret than those from molecular dynamics simulations and that high precision is readily achieved; that quasi-harmonic lattice dynamics is particularly useful at temperatures below the classical region where molecular dynamics simulations are invalid; that lattice dynamics can also be remarkably robust at elevated temperatures; and that, as discussed elsewhere,[21] it provides an extremely sensitive test for interatomic potentials, in a way that would be very difficult for molecular dynamics.

This work was supported by EPSRC grants GR/K05979 and GR/L31340. G.D.B. gratefully acknowledges financial support from la Universidad de Buenos Aires. His contribution to this work was made possible by means of a grant from el Consejo Nacional de Investigaciones Científicas y Técnicas de la República Argentina. Computational resources were also made available on the CRAY T3D at Edinburgh through SERC grant GR/K41625.

References

1 *E.g.* D. Fincham, W. C. Mackrodt and P. J. Mitchell, *J. Phys. Condens. Matter*, 1994, **6**, 393.
2 *E.g.* G. D. Barrera, M. B. Taylor, N. L. Allan, T. H. K. Barron, L. N. Kantorovich and W. C. Mackrodt, *J. Chem. Phys.*, 1997, **107**, 4337.
3 *E.g. Computer Simulation of Solids*, ed. C. R. A. Catlow and W. C. Mackrodt, Springer-Verlag, Berlin, 1982.
4 *J. Chem. Soc., Faraday Trans. 2*, 1989, **85**, 335–579.
5 *Computer Modelling in Inorganic Crystallography*, ed. C. R. A. Catlow, Academic Press, San Diego, CA, 1997.
6 Strictly constant lattice parameter in situations where the number of lattice sites changes.
7 *E.g.* N. L. Allan, W. C. Mackrodt and M. Leslie, *Adv. Ceram.*, 1987, **23**, 257.
8 S. C. Parker and G. D. Price, *Adv. Solid-State Chem*, 1989, **1**, 295.
9 A. Pavese, M. Catti, S. C. Parker and A. Wall, *Phys. Chem. Miner*, 1996, **23**, 89.
10 M. J. Gillan and P. W. M. Jacobs, *Phys. Rev. B*, 1983, **28**, 759.
11 J. H. Harding and A. M. Stoneham, *Philos. Mag. B*, 1981, **43**, 705.
12 *E.g.* J. H. Harding, *J. Chem. Soc., Faraday Trans. 2*, 1989, **85**, 351 and references therein.
13 *E.g.* C. R. A. Catlow and W. C. Mackrodt, in ref. 3, ch. 1.
14 *E.g.* D. C. Wallace, *Thermodynamics of Crystals*, Wiley, New York, 1972.
15 *E.g.* D. J. Chadi and M. L. Cohen, *Phys. Rev. B*, 1973, **8**, 5747.
16 If details of low-temperature behaviour are required, finer grids can be used as $q = 0$ is approached; see, *e.g.* T. H. K. Barron and A. Pasternak, *J. Phys. C*, 1987, **20**, 215.
17 T. H. K. Barron, T. G. Gibbons and R. W. Munn, *J. Phys. C*, 1971, **4**, 2805.
18 T. G. Gibbons, *Phys. Rev. B*, 1973, **7**, 1410.
19 A. B. Pippard, *The Elements of Classical Thermodynamics*, Cambridge University Press, Cambridge, 1964.
20 T. H. K. Barron and K. J. Rogers, *Mol. Simul.*, 1989, **4**, 27.
21 G. D. Barrera, M. B. Taylor, N. L. Allan and T. H. K. Barron, *Phys. Rev. B*, 1997, **56**, 14 380.
22 Second derivatives of the frequencies (not needed in the present application) require second-order perturbation theory. Application to ionic crystals is discussed by L. N. Kantorovich, *Phys. Rev. B*, 1995, **51**, 3520; 3535.
23 P. J. Harley, in *Numerical Algorithms*, ed., J. L. Mohamed and J. E. Walsh, Clarendon Press, Oxford, 1986, p. 239.

24 W. H. Press, S. A. Teukolsky, W. T. Vetterling and B. P. Flannery, *Numerical Recipes in Fortran*, Cambridge University Press, Cambridge, 2nd edn., 1992, p. 420.
25 N. L. Allan, M. Braithwaite, D. L. Cooper, W. C. Mackrodt and S. C. Wright, *J. Chem. Phys*., 1991, **95**, 6792.
26 C. R. A. Catlow, J. Corish, P. W. M. Jacobs and A. B. Lidiard, *J. Phys. C*, 1981, **14**, L125.
27 M. J. Gillan, *Philos. Mag. A*, 1981, **43**, 301.
28 *E.g.* J. Corish, C. R. A. Catlow and P. W. M. Jacobs, *J. Phys. Lett*., 1981, **42**, L372; P. W. M. Jacobs, J. Corish and B. A. Devlin, *Photogr. Sci. Eng*., 1982, **26**, 50.
29 The potentials are taken from the consistent set of Buckingham potentials for the alkaline-earth metal oxides given by M. J. L. Sangster and A. M. Stoneham, *Philos. Mag. B*, 1985, **52**, 717; we have extended the cut-off to 9 Å.
30 N. L. Allan, T. H. K. Barron and J. A. O. Bruno, *J. Chem. Phys*., 1996, **105**, 8300 and references therein.
31 R. M. Fracchia, G. D. Barrera, N. L. Allan, T. H. K. Barron and W. C. Mackrodt, *J. Phys. Chem. Solids*, in press.

Paper 7/01687E; *Received* 11*th March*, 1997